

Constant-pressure and constant-surface tension simulations in dissipative particle dynamics

Ask F. Jakobsen

Citation: *J. Chem. Phys.* **122**, 124901 (2005); doi: 10.1063/1.1867374

View online: <http://dx.doi.org/10.1063/1.1867374>

View Table of Contents: <http://jcp.aip.org/resource/1/JCPSA6/v122/i12>

Published by the [American Institute of Physics](#).

Additional information on *J. Chem. Phys.*

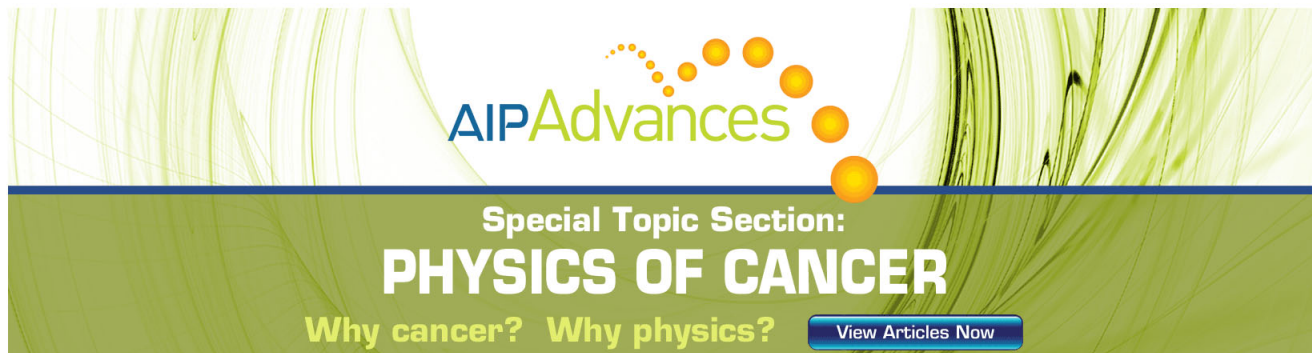
Journal Homepage: <http://jcp.aip.org/>

Journal Information: http://jcp.aip.org/about/about_the_journal

Top downloads: http://jcp.aip.org/features/most_downloaded

Information for Authors: <http://jcp.aip.org/authors>

ADVERTISEMENT



AIPAdvances

Special Topic Section:
PHYSICS OF CANCER

Why cancer? Why physics? [View Articles Now](#)

Constant-pressure and constant-surface tension simulations in dissipative particle dynamics

Ask F. Jakobsen

MEMPHYS-Center for Biomembrane Physics, Physics Department, University of Southern Denmark, Campusvej 55, DK-5230 Odense M, Denmark

(Received 14 December 2004; accepted 12 January 2005; published online 25 March 2005)

We present a method for constant-pressure and constant-surface tension simulations in dissipative particle dynamics using a Langevin piston approach. We demonstrate that the corresponding equations of motion lead to the relevant ensembles and propose an appropriate scheme of integration. After having identified a suitable set of parameters for the approach, we demonstrate the feasibility of the approach by applying it to two different systems, a simple isotropic fluid and an anisotropic fluid lipid-bilayer membrane in water. Results are presented for, respectively, isothermal bulk compressibility, tracer diffusion coefficient, lipid head-group area, and isothermal area compressibility. We find that our Langevin piston approach leads to improvements over other approaches in terms of faster equilibration and shorter correlation times of various system variables. © 2005 American Institute of Physics. [DOI: 10.1063/1.1867374]

I. INTRODUCTION

Molecular dynamics (MD) simulation in its simplest form samples the microcanonical ensemble because the basis of MD is simple Newtonian mechanics. Since the NPT ensemble is usually the physical relevant ensemble, various algorithms have been developed to perform MD simulations under constant temperature and constant pressure.^{1–3} These algorithms involve a specific coupling between the pressure and an additional variable, thereby extending the phase space of the system. These so-called extended system barostats, however, have the problem that the volume fluctuations show a “ringing” of the volume with some decay time that depends on the fictitious barostat mass. In order to shorten the decay time and to dampen out the unphysical oscillations of the volume, the Langevin piston barostat has been developed,⁴ rendering the choice of the barostat mass less critical. Whereas the extended system approach in itself is deterministic, the Langevin piston introduces stochastic dynamics into the system. The stochastic dynamics improves the effective ergodicity of the simulations⁵ which is necessary in order to extract ensemble averages from the MD simulations. In addition, the Langevin dynamics has the potential of reducing correlation times. Combining the Langevin piston with standard Langevin dynamics for the particles (thus coupling to a heat bath) has been shown to improve ergodicity and shorten correlation times.^{6,7}

Dissipative particle dynamics (DPD) simulation^{8,9} has in recent years emerged as a novel numerical technique to study soft matter and complex fluids at a large range of length and time scales. DPD is a stochastic method useful to simulate coarse-grained models of fairly complex systems involving a large number of particles. In contrast to stochastic Monte Carlo simulation, DPD has the advantage that it preserves the hydrodynamic modes, and the equilibration is much

faster than in molecular dynamics. Examples of systems that have successfully been studied by DPD include colloids,¹⁰ vesicles,¹¹ and biological membranes.^{12,13}

However, DPD is not without its problems. First of all, the integration of the equations of motion of DPD is highly nontrivial.^{14–16} Whereas inappropriate integration in MD, e.g., augmented by using too large time steps, usually manifests itself in some easily detectable and incorrect system behavior, integration of the DPD equations of motion may lead to unphysical and subtle artifacts that are not easily detected. This is, in particular, the case when adding an extended system barostat or Langevin piston to the DPD integration routine. This is the problem we will address in the present paper. In particular, we will establish DPD methods for sampling the NPT ensemble for an isotropic fluid and the $NP_N\gamma_S T$ ensemble for an anisotropic fluid, where P_N is the normal pressure and γ_S is an interfacial tension.

The constant-normal pressure and constant-surface tension ensemble, $NP_N\gamma_S T$, is relevant for interfacial systems such as fluid lipid-bilayer membranes in water. When modeling lipid bilayers it is important to be able to apply a specific surface tension. Especially the tensionless membrane is of interest since it is believed that a self-assembled membrane has zero surface tension. A method for accomplishing constant surface tension in DPD involves combining DPD with a Monte Carlo algorithm for updating the size of the simulation box every now and then in an abrupt and stochastic way.¹⁷ By this method, the normal pressure is not an independent variable since the volume of the box is fixed. Moreover, the problem remains as to how often one should perform a Monte Carlo step to update the simulation box size. Other workers have found the tensionless state of model lipid membranes by trial and error within the canonical ensemble.¹³

In the following, a systematic method for sampling the NPT and the $NP_N\gamma_S T$ ensembles in DPD will be established.

The equations of motion will be shown to produce the right ensembles. An algorithm for integrating the equations will be presented. The feasibility of the methods is tested on two well-known systems. For testing the NPT ensemble simulations we use a simple DPD fluid. For testing the $NP_N\gamma_S T$ ensemble simulations we consider a model lipid-bilayer system which is an anisotropic fluid.

II. DISSIPATIVE PARTICLE DYNAMICS

In DPD the total force on particle i at position \mathbf{r}_i and with momentum \mathbf{p}_i is given by

$$\dot{\mathbf{p}}_i = \mathbf{F}_i^C + \sum_{j \neq i} \mathbf{F}_{ij}^D + \sum_{j \neq i} \mathbf{F}_{ij}^R, \quad (1)$$

where \mathbf{F}_i^C is a conservative force exerted on particle i from particle j . The dissipative force \mathbf{F}_{ij}^D and the random force \mathbf{F}_{ij}^R have the form

$$\mathbf{F}_{ij}^D = -\gamma\omega_D(r_{ij})(\mathbf{e}_{ij} \cdot \mathbf{v}_{ij})\mathbf{e}_{ij}, \quad (2)$$

$$\mathbf{F}_{ij}^R = \sigma\omega_R(r_{ij})\xi_{ij}\mathbf{e}_{ij}, \quad (3)$$

where $\mathbf{r}_{ij} = \mathbf{r}_i - \mathbf{r}_j$, $r_{ij} = |\mathbf{r}_{ij}|$, $\mathbf{e}_{ij} = \mathbf{r}_{ij}/r_{ij}$, and $\mathbf{v}_{ij} = \mathbf{v}_i - \mathbf{v}_j$, where \mathbf{v}_i is the velocity of particle i , and ω_D and ω_R are arbitrary weight functions.

The variable ξ_{ij} represent Gaussian white noise with $\xi_{ij} = \xi_{ji}$ and the following stochastic properties:

$$\begin{aligned} \langle \xi_{ij}(t) \rangle &= 0, \\ \langle \xi_{ij}(t)\xi_{i'j'}(t') \rangle &= (\delta_{ii'}\delta_{jj'} + \delta_{ij'}\delta_{ji'})\delta(t-t'). \end{aligned} \quad (4)$$

The parameter γ controls the strength of the dissipation and the parameter σ the strength of the noise. The thermostat consisting of the random and dissipative forces in Eq. (1) conserves momentum pairwise, so DPD is a momentum-conserving thermostat.

It has been proved that the corresponding Fokker–Planck equation of Eq. (1) has the canonical equilibrium distribution as a solution given the following constraints:⁹

$$[\omega_R(r)]^2 = \omega_D(r), \quad (5a)$$

$$\sigma^2 = 2k_B T \gamma. \quad (5b)$$

The above is thus a fluctuation-dissipation theorem for the DPD system.

In DPD simulations $\omega_D(r)$ is often chosen to be

$$\omega_D(r) = \begin{cases} 1 - r/r_0, & r < r_0 \\ 0, & r \geq r_0 \end{cases}, \quad (6)$$

where r_0 is the cutoff distance.

A conservative soft-core repulsion is usually modeled simply by

$$\mathbf{F}_{ij}^S = \mathcal{A}_{ij}\omega_D(r_{ij})\mathbf{e}_{ij}, \quad (7)$$

where ω_D is chosen as in Eq. (6). The repulsion parameter \mathcal{A}_{ij} gives different particle/bead species their identity. To create model polymers, beads are tied together by harmonic springs, and to add rigidity to the structure, angle-bending potentials are applied.

All beads have the same mass m_0 and cutoff r_0 (effective size). The energy scale is set by $k_B T$. We will use units where all these quantities are unity. From m_0 , r_0 , and $k_B T$, a time scale $t_0 = \sqrt{m_0 r_0^2 / k_B T}$ can be extracted, and in the following all time scales will be in this DPD time unit.

The DPD particles are simulated in a box with periodic boundary conditions. In the case of the isotropic fluid, the appropriate choice of box shape is that of a cube whose volume changes by keeping the shape fixed. Since the bilayers we are interested in are also fluids, they cannot resist shear. Therefore the appropriate simulation box has the shape of an orthorhombic cell, i.e., all normals to the faces of the simulation box point along the canonical coordinate axes.

III. CUBIC BOX

The equations of motions for a d -dimensional cubic simulation box containing N particles and $N_f = dN - d \approx dN$ degrees of freedom are the following:

$$\dot{\mathbf{r}}_i = \frac{\mathbf{p}_i}{m_i} + \frac{p_\epsilon}{W}\mathbf{r}_i, \quad (8a)$$

$$\begin{aligned} \dot{\mathbf{p}}_i &= \mathbf{F}_i^C - \sum_{j \neq i} \gamma\omega_D(r_{ij})(\mathbf{e}_{ij} \cdot \mathbf{v}_{ij})\mathbf{e}_{ij} \\ &+ \sum_{j \neq i} \sigma\omega_R(r_{ij})\xi_{ij}\mathbf{e}_{ij} - \left(1 + \frac{d}{N_f}\right)\frac{p_\epsilon}{W}\mathbf{p}_i, \end{aligned} \quad (8b)$$

$$\dot{\mathcal{V}} = \frac{d\mathcal{V}p_\epsilon}{W}, \quad (8c)$$

$$\dot{p}_\epsilon = d\mathcal{V}[\mathcal{P}(t) - P_0] + \frac{d}{N_f} \sum_i \frac{p_i^2}{m_i} - \gamma_p p_\epsilon + \sigma_p \xi_p, \quad (8d)$$

where ξ_{ij} has the property as defined in Eq. (4) and ξ_p is Gaussian white noise with the properties $\langle \xi_p \rangle = 0$ and $\langle \xi_p(t)\xi_p(t') \rangle = \delta(t-t')$. The piston “momentum” is denoted p_ϵ , \mathcal{V} is the simulation box volume, W is the piston “mass,” P_0 is the target pressure, and d is the dimensionality of the simulation system. It is called the extended system method when $\gamma_p = \sigma_p = 0$, since volume and volume momentum have been coupled to the equations of motion. When γ_p and σ_p is larger than zero, the method is called the Langevin piston method. Later we will find the exact relation between γ_p and σ_p . So far we will assume that $\sigma_p \rightarrow 0$ when $\gamma_p \rightarrow 0$.

The instantaneous pressure $\mathcal{P}(t)$ is defined as

$$\mathcal{P}(t) = \frac{1}{d\mathcal{V}} \left[\sum_i \frac{p_i^2}{m_i} + \sum_i \mathbf{F}_i^C \cdot \mathbf{r}_i \right], \quad (9)$$

where \mathcal{V} is the volume of the simulation box. Notice that this is not the instantaneous pressure calculated from the virial equation, since the stochastic part is not included in Eq. (9).

In the limit $\gamma \rightarrow 0$ and $\gamma_p \rightarrow 0$, it is straightforward to show that the dynamical system conserves the quantity

$$H' = \mathcal{H}(\mathbf{r}^N, \mathbf{p}^N) + P_0 \mathcal{V} + \frac{p_\epsilon^2}{2W}, \quad (10)$$

where \mathcal{H} is the Hamiltonian of the particle subsystem. The energy function H' will be referred to as the extended system energy. Note that H' is not a Hamiltonian since Eqs. (8a)–(8d) cannot be retrieved as derivatives of H' . The compressibility κ of the extended phase space as defined in Ref. 18 is given by

$$\kappa = \sum_i \nabla_{\mathbf{r}_i} \cdot \dot{\mathbf{r}}_i + \sum_i \nabla_{\mathbf{p}_i} \cdot \dot{\mathbf{p}}_i + \frac{\partial}{\partial p_\epsilon} \dot{p}_\epsilon + \frac{\partial}{\partial \mathcal{V}} \dot{\mathcal{V}} = 0. \quad (11)$$

One can think of Eqs. (8a)–(8d) as a coordinate transformation of the extended phase space, and the Jacobian J of this coordinate transformation is found to be $J=1$ (Ref. 2) since

$$\frac{dJ}{dt} = \kappa J. \quad (12)$$

Thus the phase space has a constant unit metric $\sqrt{g}=1$ and the dynamical system obeys the Liouville theorem,^{18,19}

$$\frac{\partial \rho}{\partial t} + \sum_i \dot{\mathbf{r}}_i \cdot \nabla_{\mathbf{r}_i} \rho + \sum_i \dot{\mathbf{p}}_i \cdot \nabla_{\mathbf{p}_i} \rho + \dot{p}_\epsilon \frac{\partial \rho}{\partial p_\epsilon} + \dot{\mathcal{V}} \frac{\partial \rho}{\partial \mathcal{V}} = 0. \quad (13)$$

One can justify that Eqs. (8a)–(8d) in the particle subsystem actually sample the isothermal-isobaric ensemble in the limit $\gamma \rightarrow 0$ and $\gamma_p \rightarrow 0$. The phase-space probability density for the extended system is given by

$$\rho_{NPH'}(\mathbf{r}^N, \mathbf{p}^N, p_\epsilon, \mathcal{V}) \propto \frac{\delta(H' - H_0^i)}{\Omega_{NPH'}(\mathbf{r}^N, \mathbf{p}^N, p_\epsilon, \mathcal{V})}. \quad (14)$$

The probability density of the extended system when coupled to a heat bath is given by

$$\rho_{NPT}(\mathbf{r}^N, \mathbf{p}^N, p_\epsilon, \mathcal{V}) \propto \frac{\exp(-H'/k_B T)}{\Omega_{NPT}(\mathbf{r}^N, \mathbf{p}^N, p_\epsilon, \mathcal{V})}. \quad (15)$$

The integration over the barostat momentum p_ϵ gives a constant and hence,

$$\rho_{NPT}(\mathbf{r}^N, \mathbf{p}^N, \mathcal{V}) \propto \frac{1}{\Omega_{NPT}(\mathbf{r}^N, \mathbf{p}^N, \mathcal{V})} \times \exp\left(-\frac{\mathcal{H}(\mathbf{r}^N, \mathbf{p}^N) + P\mathcal{V}}{k_B T}\right), \quad (16)$$

which precisely is the phase-space probability density for the isobaric-isothermal ensemble.

Equations (8a)–(8d) can be put onto a mathematically well-defined form for stochastic differential equations which makes it straightforward to apply the standard procedures for finding the associated Fokker–Planck equation.²⁰ Equations (8b) and (8d) have stochastic elements and require special attention. In the stochastic terms the differentials are replaced by stochastic differentials,

$$d\mathbf{p}_i = \left[\mathbf{F}_i^C - \sum_{j \neq i} \gamma \omega_D(r_{ij}) \left(\mathbf{e}_{ij} \cdot \left\{ \frac{\mathbf{p}_i}{m_i} - \frac{\mathbf{p}_j}{m_j} \right\} \right) \mathbf{e}_{ij} \right] dt + \sum_{j \neq i} \sigma \omega_R(r_{ij}) \mathbf{e}_{ij} dW_{ij} - \left(1 + \frac{d}{N_f} \right) \frac{p_\epsilon}{W} \mathbf{p}_i dt, \quad (17)$$

$$dp_\epsilon = \left[d\mathcal{V}[\mathcal{P}(t) - P_0] + \frac{d}{N_f} \sum_i \frac{p_i^2}{m_i} - \gamma_p p_\epsilon \right] dt + \sigma_p dW,$$

where dW and $dW_{ij} = dW_{ji}$ are independent increments of the Wiener process with the latter having the property

$$dW_{ij} dW_{i'j'} = (\delta_{ii'} \delta_{jj'} + \delta_{ij'} \delta_{ji'}) dt. \quad (18)$$

Both dW and dW_{ij} are infinitesimals of order 1/2. The Fokker–Planck equation that corresponds to the stochastic differential equations (8a)–(8d) is

$$\begin{aligned} \frac{\partial \rho}{\partial t} + \sum_i \left(\frac{\mathbf{p}_i}{m_i} + \frac{p_\epsilon}{W} \mathbf{r}_i \right) \cdot \nabla_{\mathbf{r}_i} \rho + \sum_i \left[\mathbf{F}_i^C - \left(1 + \frac{d}{N_f} \right) \frac{p_\epsilon}{W} \mathbf{p}_i \right] \\ \times \nabla_{\mathbf{p}_i} \rho + \left[d\mathcal{V}[\mathcal{P}(t) - P_0] + \frac{d}{N_f} \sum_i \frac{p_i^2}{m_i} \right] \frac{\partial \rho}{\partial p_\epsilon} + \dot{\mathcal{V}} \frac{\partial \rho}{\partial \mathcal{V}} \\ = \sum_{i,j \neq i} \mathbf{e}_{ij} \cdot \nabla_{\mathbf{p}_i} \left[\gamma \omega_D \left(\mathbf{e}_{ij} \cdot \left\{ \frac{\mathbf{p}_i}{m_i} - \frac{\mathbf{p}_j}{m_j} \right\} \right) \right] \\ + \frac{\sigma^2}{2} \omega_R^2 \mathbf{e}_{ij} \cdot (\nabla_{\mathbf{p}_i} - \nabla_{\mathbf{p}_j}) \left[\rho + \frac{\partial}{\partial p_\epsilon} \left[\gamma_p p_\epsilon + \frac{\sigma_p^2}{2} \frac{\partial}{\partial p_\epsilon} \right] \rho \right]. \end{aligned} \quad (19)$$

The isothermal-isobaric probability density ρ_{NPT} must be a solution to Eq. (19). It is straightforward to show that the left-hand side is zero. The right-hand side is zero for the choice

$$\sigma_p^2 = 2\gamma_p W k_B T \quad (20)$$

and the constraints in Eqs. (5a) and (5b) being satisfied.

IV. ORTHORHOMBIC BOX

The Parrinello–Rahman method for a fully flexible simulation box is given in Ref. 3 (slightly modified in Ref. 2),

$$\begin{aligned} \dot{\mathbf{r}}_i &= \frac{\mathbf{p}_i}{m_i} + \frac{\mathbf{p}_g}{W_g} \mathbf{r}_i, & \dot{\mathbf{p}}_i &= \mathbf{F}_i^C - \frac{\mathbf{p}_g}{W_g} - \frac{1}{N_f} \frac{\text{Tr}[\mathbf{p}_g]}{W_g} \mathbf{p}_i, \\ \dot{\mathbf{h}} &= \frac{\mathbf{p}_g \mathbf{h}}{W_g}, & \dot{\mathbf{p}}_g &= \mathcal{V}(\mathbf{p} - P_0 \mathbf{I}) + \left[\frac{1}{N_f} \sum_i \frac{p_i^2}{m_i} \right] \mathbf{I}, \end{aligned} \quad (21)$$

where \mathbf{h} is a matrix with the columns given by the edges of the simulation box and the pressure tensor \mathbf{p} is defined as

$$P_{\alpha\beta} = \frac{1}{\mathcal{V}} \left[\sum_i \frac{(\mathbf{p}_i)_\alpha (\mathbf{p}_i)_\beta}{m_i} + (\mathbf{F}_i)_\alpha (\mathbf{r}_i)_\beta \right]. \quad (22)$$

Equation (21) conserves the quantity

$$H' = \mathcal{H}(\mathbf{r}^N, \mathbf{p}^N) + \frac{\text{Tr}[\mathbf{p}_g^T \mathbf{p}_g]}{2W_g} + P_0 \det[\mathbf{h}], \quad (23)$$

where $\mathcal{V} = \det(\mathbf{h})$.

The compressibility κ of the extended phase space of Eq. (21) is nonzero. The Parrinello–Rahman method was developed for anisotropic solids. Therefore the simulation box can change shape and size. Since DPD deals with complex fluid systems that cannot resist shear forces we do not need the simulation box to change shape. Thus it is sufficient to work with an orthorhombic box (all edges of the simulation box point along the coordinate axis). The advantage is that $\kappa=0$ if we restrict the simulation box to be an orthorhombic box.

One can derive the equations for the isotropic simulation box by assuming that $h_{\alpha\beta}=\mathcal{V}^{1/3}\delta_{\alpha\beta}$ and $P_{\alpha\beta}=\mathcal{P}\delta_{\alpha\beta}$. Similarly one can find the equations for an orthorhombic simulation box by demanding that \mathbf{h} is zero off-diagonal and that only the entries along the diagonal of Eq. (21) are included.

The proposed equations for the orthorhombic box are

$$\dot{r}_{i,\alpha} = \frac{p_{i,\alpha}}{m_i} + \frac{p_{g,\alpha}}{W_g} r_{i,\alpha}, \quad (24a)$$

$$\begin{aligned} \dot{p}_{i,\alpha} = & F_{i,\alpha} - \frac{p_{g,\alpha}}{W_g} p_{i,\alpha} - \frac{1}{N_f} \frac{\text{Tr}[\mathbf{p}_g]}{W_g} p_{i,\alpha} - \sum_{j \neq i} \gamma \omega_D(r_{ij}) \\ & \times (\mathbf{e}_{ij} \cdot \mathbf{v}_{ij})(\mathbf{e}_{ij})_\alpha + \sum_{j \neq i} \sigma \omega_R(r_{ij}) \xi_{ij}(\mathbf{e}_{ij})_\alpha, \end{aligned} \quad (24b)$$

$$\dot{L}_\alpha = \frac{p_{g,\alpha} L_\alpha}{W_g}, \quad (24c)$$

$$\dot{p}_{g,\alpha} = \mathcal{V}(P_\alpha - P_0) + \frac{1}{N_f} \sum_i \frac{p_i^2}{m_i} - \gamma_p p_{g,\alpha} + \sigma_p \xi_{p,\alpha}, \quad (24d)$$

where $h_\alpha = h_{\alpha\alpha}$, $P_\alpha = P_{\alpha\alpha}$, $p_{g,\alpha} = (p_g)_{\alpha\alpha}$, and L_α for $\alpha = \{x, y, z\}$ is the length of the simulation box in the α direction. The volume is given by $\mathcal{V} = L_x L_y L_z$. It should be noted that there is no summation over repeated indices.

A. Constant-surface tension

Equations (24a)–(24d) ensure that $\langle P_\alpha \rangle = P_0$. The surface tension γ_S for an interfacial system in the xy plane is given by

$$\gamma_S = \langle L_z \times [P_z - \frac{1}{2}(P_x + P_y)] \rangle, \quad (25)$$

where L_z is the dimension of the simulation box in the z direction, that is, perpendicular to the interface. Hence, the above equations for the orthorhombic box lead to zero surface tension.

If we want to impose constant-surface tension and constant-normal pressure ($NP_N \gamma_S T$ ensemble) we need to invoke an anisotropic pressure tensor in such a way that the desired values of γ_S^0 and P_N^0 are obtained. Choosing the correct anisotropic target pressure tensor leads to the following changes of the first term of the right-hand side of Eq. (24d):

$$\dot{p}_{g,\alpha} = A[\gamma_S^0 - h_z(P_N^0 - P_\alpha)] + \dots, \quad (26)$$

$$\dot{p}_{g,z} = \mathcal{V}(P_z - P_N^0) + \dots, \quad (27)$$

where $\alpha = \{x, y\}$ and A is the area in the xy plane. For $\gamma_S^0 = 0$ we retrieve Eqs. (24a)–(24d).

V. INTEGRATION

We now describe the integration scheme first in the case of the cubic box system. This scheme can readily be extended to the case of the orthorhombic box system.

Since DPD involves momentum-conserving Langevin dynamics one is often, as in standard Langevin dynamics, tempted to use too large a time step Δt . This may go unnoticed since the total energy does not diverge in DPD even for a large number of time steps. Without Langevin dynamics, the total energy would blow up quickly if the time step is too large. Moreover, since DPD typically is applied to particle systems with soft potentials, the undesired effects of using too large a time step are often even more subtle. The result of using too large a time step can be various artifacts in the physical properties of the system which turn out to depend strongly on the size of Δt . For example, there may be a deviation of $\langle k_B T \rangle_i$ from the value of $k_B T$ that appears in Eq. (5b) and this deviation may depend on the magnitude of Δt .

A host of different integration schemes exist with different merits and of varying complexity. The standard algorithm of DPD is the DPD-velocity-Verlet integration scheme.^{14,15} In this algorithm the problem, that the dissipative forces in DPD depend on the velocities, is addressed by using intermediate velocities (a sort of “prediction step”) for the dissipative forces. The DPD-velocity-Verlet algorithm is preferred because of its simplicity, speed, and robustness. Furthermore it is relatively straightforward to include the extended system barostat or the Langevin piston into this algorithm.

When $\gamma = \gamma_p = 0$, Eqs. (8a)–(8d) can be propagated using the standard velocity-Verlet algorithm. The equations are complicated by the fact that the new particle velocities depend on the new v_ϵ and vice versa. This problem can be conveniently solved quite simply by using an iterative procedure.²

Combining the DPD-velocity-Verlet integration scheme with the iterative procedure leads to the following algorithm:

$$v_\epsilon'' \leftarrow v_\epsilon' \quad v_\epsilon' \leftarrow v_\epsilon \quad \epsilon' \leftarrow \epsilon$$

$$\mathbf{v}_i \leftarrow \mathbf{v}_i + \frac{1}{2} \left\{ \left(\frac{\mathbf{F}_i^C}{m_i} + \frac{\mathbf{F}_i^D}{m_i} - 2v_\epsilon \mathbf{v}_i \right) \Delta t + \frac{\mathbf{F}_i^R}{m_i} \sqrt{\Delta t} \right\}$$

$$v_\epsilon \leftarrow v_\epsilon + \frac{1}{2} \frac{F_\epsilon}{W} \Delta t$$

$$\epsilon \leftarrow \epsilon + v_\epsilon \Delta t$$

$$\mathbf{r}_i \leftarrow \exp(\epsilon - \epsilon') \{ \mathbf{r}_i + \mathbf{v}_i \Delta t \}$$

Update the volume \mathcal{V}

Compute the forces \mathbf{F}_i^C ,

\mathbf{F}_i^D , and \mathbf{F}_i^R

Find the pressure \mathcal{P}

$$\tilde{\mathbf{v}}_i \leftarrow \mathbf{v}_i \quad \tilde{v}_\epsilon \leftarrow v_\epsilon$$

$$v_\epsilon \leftarrow v_\epsilon'' + 2 \frac{F_\epsilon}{W} \Delta t \quad (\text{initial guess of } v_\epsilon)$$

$$\mathbf{v}_i \leftarrow \frac{\exp(\epsilon - \epsilon') \tilde{\mathbf{v}}_i + \frac{1}{2} \left\{ \left(\frac{\mathbf{F}_i^C}{m_i} + \frac{\mathbf{F}_i^D}{m_i} \right) \Delta t + \frac{\mathbf{F}_i^R}{m_i} \sqrt{\Delta t} \right\}}{1 + v_\epsilon \Delta t} \quad (28a)$$

$$\text{Find } F_\epsilon = F_\epsilon(\mathbf{v}_i, v_\epsilon, \mathcal{V}, \mathcal{P}) \quad (28b)$$

$$v_\epsilon \leftarrow \tilde{v}_\epsilon + \frac{1}{2} \frac{F_\epsilon}{W} \Delta t. \quad (28c)$$

The steps in Eqs. (28a)–(28c) are iterated to convergence which happens very fast. Typically four to five iterations are sufficient. The barostat force F_ϵ is defined as the right-hand side of Eq. (8d). Notice that the iteration does not require any evaluation of the (nonbonded) forces which is the most time consuming part of the above algorithm. In the limit $W \rightarrow \infty$ the above algorithm is identical to the DPD-velocity-Verlet algorithm. For $\gamma = \sigma = 0$ the algorithm is identical to the velocity-Verlet algorithm of Ref. 2. Furthermore one should notice that the particle coordinates need no additional rescaling.

The above integration scheme described above for the case of a cubic simulation box can readily be extended to apply to the orthorhombic box system.

VI. TWO CASE STUDIES

We now turn to the application of our DPD Langevin piston approach described above to two specific systems, a simple isotropic fluid and an anisotropic fluid lipid-bilayer membrane in waterlike solvent. First we have to determine the appropriate parameters of the applied algorithms.

A. Choice of parameters

The parameters W and γ_p have to be chosen carefully in order to achieve efficient sampling without disturbing the physical system. For the cubic simulation box, the fictitious barostat mass should be chosen as²¹

$$W = (N_f + d) k_B T \tau_p^2, \quad (29)$$

where characteristic time of the barostat τ_p should be chosen slightly larger than the smallest time scale of the particle motions. The power spectrum of various physical quantities should not change when the pressure coupling is applied.

If τ_p is chosen too large, the barostat will effectively decouple from the particle system which leads long correlation times and inefficient sampling. If τ_p is chosen too small, the coupling between the box and the particles gets too strong involving the danger of disturbing the essential dynamics. On the other hand, the advantage is short correlation times. The Langevin piston method makes it possible to use a large τ_p and still have short correlation times. The appropriate range of τ_p can often be found from knowledge of the dynamics of the studied system. By trial and error one then adjusts the parameters such that the barostat has minimum impact on the system and the equilibration time is tolerable.

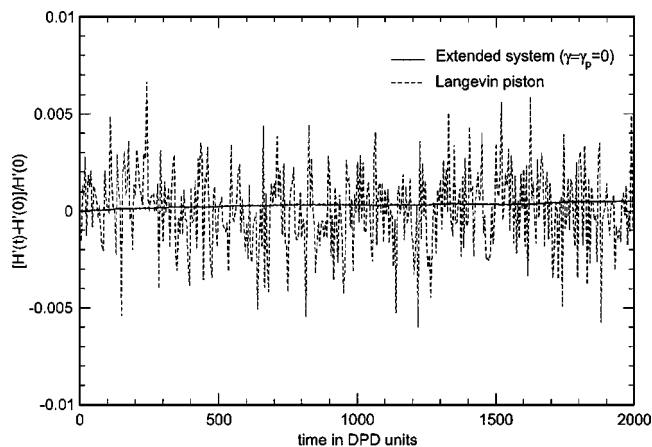


FIG. 1. The extended energy $H'(t)$ as defined in Eq. (10) for a simple fluid with $\mathcal{A}_{ij} = 25k_B T$. The total number of integration steps is 200 000.

The choice of γ_p is of less importance since the effect of the Langevin dynamics is small on the particle system in equilibrium. However, a clever choice γ_p can significantly reduce the equilibration time by avoiding “ringing” of the pressure and by leading to a fast exponential approach to the reference pressure. As a rule of thumb γ_p should be between $2/\tau_p$ and $10/\tau_p$.

For the orthorhombic system the barostat mass W_g should be chosen to be²¹

$$W_g = (N_f + d) k_B T \tau_p^2 / d. \quad (30)$$

The same criteria for choosing τ_p and γ_p apply as for the cubic simulation box.

B. Simple fluid

To test the proposed equations of motion for the isotropic simulation box we consider a simple DPD fluid. Simple means that only one bead species is present and the only interaction is the nonbonded soft-core repulsion in Eq. (6) with the standard choice of the parameter $\mathcal{A}_{ij} = 25k_B T$. The simulation box size is initially $\mathcal{V} = (10r_0)^3$ containing 3000 beads. The simulations were run for 2×10^5 time steps. The target pressure P_0 was set to $23.649k_B T / r_0^3$, which gives approximately the same average box size as the initial box. The extended system barostat time was set to $\tau_p = 2$ and the Langevin piston parameter to $\gamma_p = 10/\tau_p = 5$. The reason for choosing this value of τ_p is the fact that the fastest time scale in the model lipid bilayer is ≈ 0.5 due to bond stretching and angle bending in the lipid tails.

The extended system energy H' drifts 0.03% during 10^5 steps with a time step of $\Delta t = 0.01$ when $\gamma = \gamma_p = 0$. When adding DPD and the Langevin piston we expect H' to fluctuate but without any overall drift. This is indeed the case as demonstrated in Fig. 1. The drawback of using Langevin dynamics is of course that the consistency of the simulation algorithm cannot be checked via a criterion of energy conservation.

The average volume is found to be $\langle \mathcal{V} \rangle = (1000.3 \pm 0.1)r_0^3$. For the parameters values chosen, the vol-

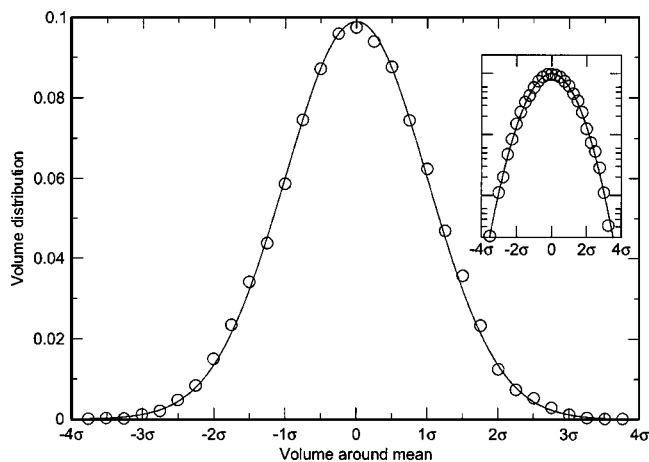


FIG. 2. Probability distribution of the volume fluctuations.

ume fluctuations are found to be Gaussian as seen in Fig. 2. The volume fluctuations are related to the isothermal compressibility β_T by

$$\langle \delta V^2 \rangle = \mathcal{V} k_B T \beta_T \quad (31)$$

and the dimensionless compressibility β is given by $\beta = \rho k_B T \beta_T$, where ρ is the number density. For $T=300$ K and with the given choice of soft repulsion parameter $\mathcal{A} = 25k_B T$, we find $\beta^{-1} = 16.1 \pm 1.0$. The parameter $\mathcal{A} = 25k_B T$ was chosen in Ref. 22 in such a way that the simple fluid has the compressibility of water ($\beta^{-1} \approx 16$). Hence, the result obtained from our Langevin piston approach is in full agreement with this finding.

The power spectrum of the temperature is shown in Fig. 3. The power spectrum is found to exhibit peaks that correspond to the values chosen for τ_p . These peaks are removed by the Langevin piston. Using only DPD (no barostat) the average temperature $\langle k_B T \rangle_t = 0.9996 \pm 0.0007$ and with the Langevin piston $\langle k_B T \rangle_t = 0.9996 \pm 0.0006$. For the extended system $\langle k_B T \rangle_t = 0.9991 \pm 0.0006$. It is seen that the barostat methods do not contribute to the integrator-induced deviation

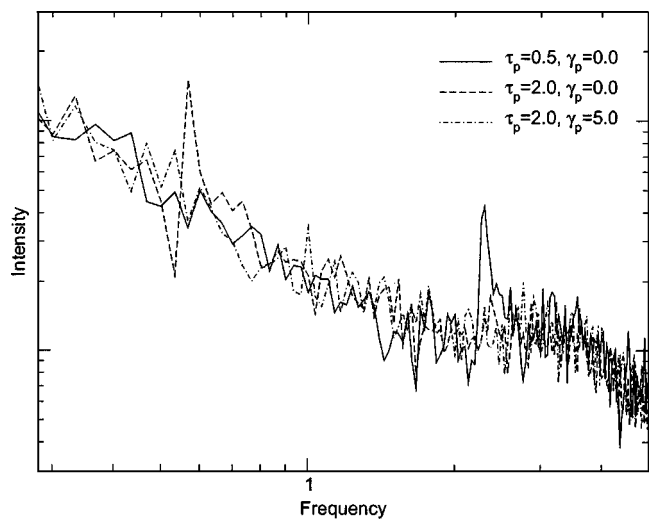


FIG. 3. Power spectrum of the kinetic temperature for the simple fluid. The spectrum has been smoothed with a Savitsky-Golay filter.

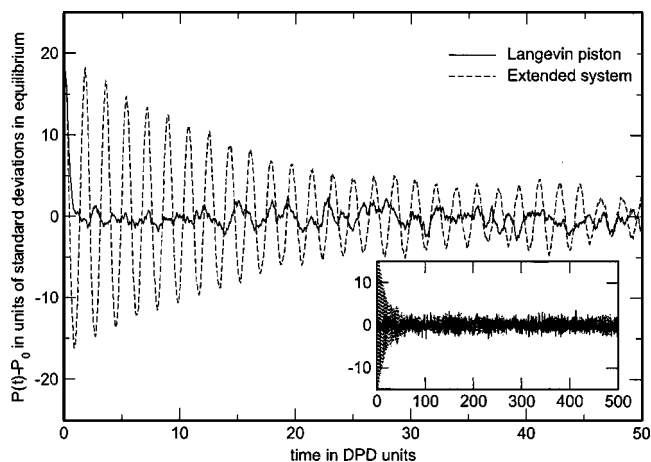


FIG. 4. Equilibration of the pressure when the system is prepared in a state far from equilibrium.

of $\langle k_B T \rangle_t$ from the choice of $k_B T$ made in Eq. (5b). The temperature fluctuations are not affected by the barostat methods.

A clear advantage of our Langevin piston approach can be seen if the box is started far from equilibrium as illustrated in Fig. 4 which shows the equilibration of the pressure. The autocorrelation analysis in equilibrium of the pressure in Fig. 5 shows that with the choice of $\gamma_p = 10/\tau_p$ the equilibration is of the order 50–100 times as fast.

To further test our Langevin piston approach, we calculated a single-particle property of the system being the tracer diffusion coefficient D , which was determined to be $D = 0.29$ in units of r_0^2 per DPD unit time step. This value was found not to be influenced by applying the pressure coupling.

C. Bilayer model

The parameters for the model bilayer were taken from Ref. 13. Each lipid consists of 15 beads, three hydrophilic head-group beads (H), and two chains consisting of each 6 beads (T) that are hydrophobic. A waterlike solvent is modeled by a single water bead (W). In Table I the parameters for the nonbonded interactions are listed. The DPD noise param-

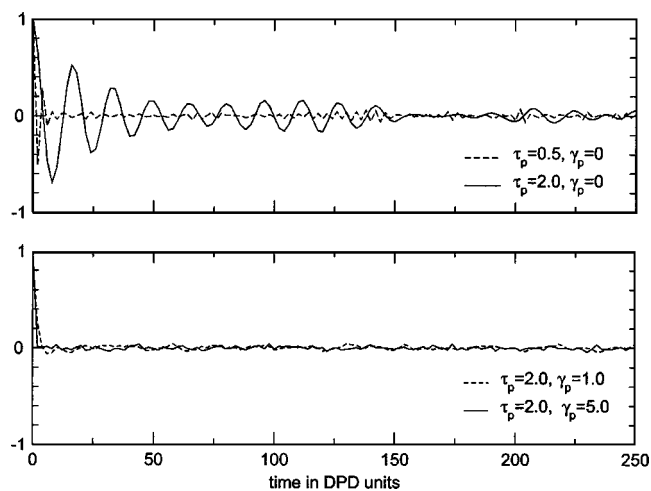


FIG. 5. Autocorrelation of the pressure for the simple DPD fluid.

TABLE I. The nonbonded soft interactions from Ref. 13. The head bead is denoted by H , the tail bead by T , and the water bead by W .

Bead pair	$A_{ij}(k_B T)$
$H-H$	25
$T-T$	25
$W-W$	25
$H-W$	35
$H-T$	50
$T-W$	75

eter σ is set to 3 and the dissipation parameter $\gamma=9/2$ for $k_B T=1$. The harmonic bond potential is given by

$$U_2(\mathbf{r}_i, \mathbf{r}_{i+1}) = \frac{1}{2} k_2 (|\mathbf{r}_{i,i+1}| - l_0)^2,$$

where l_0 is the equilibrium distance between two consecutive bonds in the lipid tails. The bond parameters $l_0=0.5r_0$ and $k_2=128k_B T/r_0^2$ are used in the following. The bond bending potential used is defined as

$$U_3(\mathbf{r}_{i-1}, \mathbf{r}_i, \mathbf{r}_{i+1}) = k_3 [1 - \cos(\phi - \phi_0)],$$

where ϕ_0 is the equilibrium angle between three consecutive bonds. The angle ϕ is defined as

$$\cos \phi = \frac{\mathbf{r}_{i-1,i} \cdot \mathbf{r}_{i,i+1}}{|\mathbf{r}_{i-1,i}| |\mathbf{r}_{i,i+1}|}.$$

In the following the parameters used are $\phi_0=0$ and $k_3=20k_B T$. The simulation box volume is initially $\mathcal{V}=(32r_0)^3$ containing 98 304 beads and the number of model lipids is 1688, and there are $\approx 73\,000$ water beads. The lipids spontaneously self-assemble to form a bilayer as seen in Fig. 6. This gives approximately a tensionless membrane.

The extended system energy H' is conserved within 0.03% after 10^5 time steps when $\gamma=\gamma_p=0$. The pressure and volume fluctuations in the extended system barostat and the

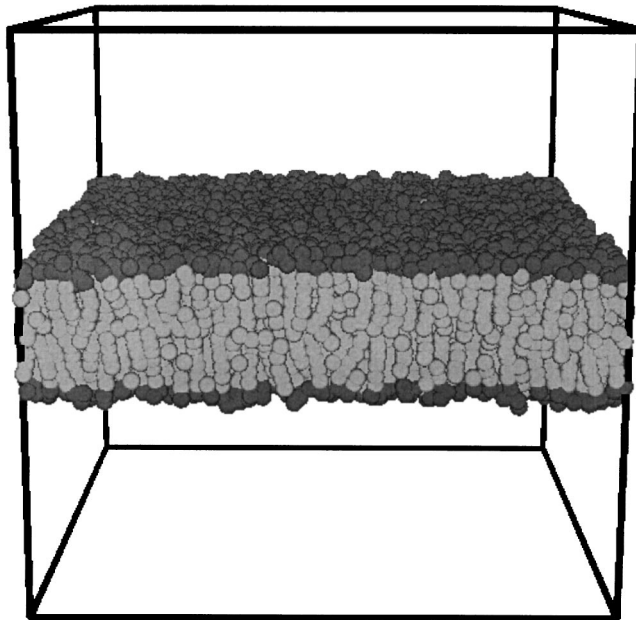


FIG. 6. The bilayer model of Shillcock and Lipowsky. The dark beads represent the lipid head group and the light beads represent the carbons along the lipid tails.

Langevin piston method are found to be indistinguishable. For both pressure-coupled systems the average kinetic temperature and the fluctuations of the kinetic temperature are the same as with the system only being thermostated by DPD.

In the following the surface tension is given in units of $k_B T/r_0^2$. The surface tension is found to be $\gamma_S=(0.00\pm 0.05)$ for the extended system barostat and -0.02 ± 0.08 for the Langevin piston. The instantaneous surface tension, autocorrelation analysis, and the box dimensions are shown on Fig. 7. The average area per lipid is found to be $(1.2079\pm 0.0005)r_0^2$ which is 0.6% below what was found in Ref. 13. The area compressibility modulus K_A can be found from the fluctuations in the area (Refs. 23 and 24),

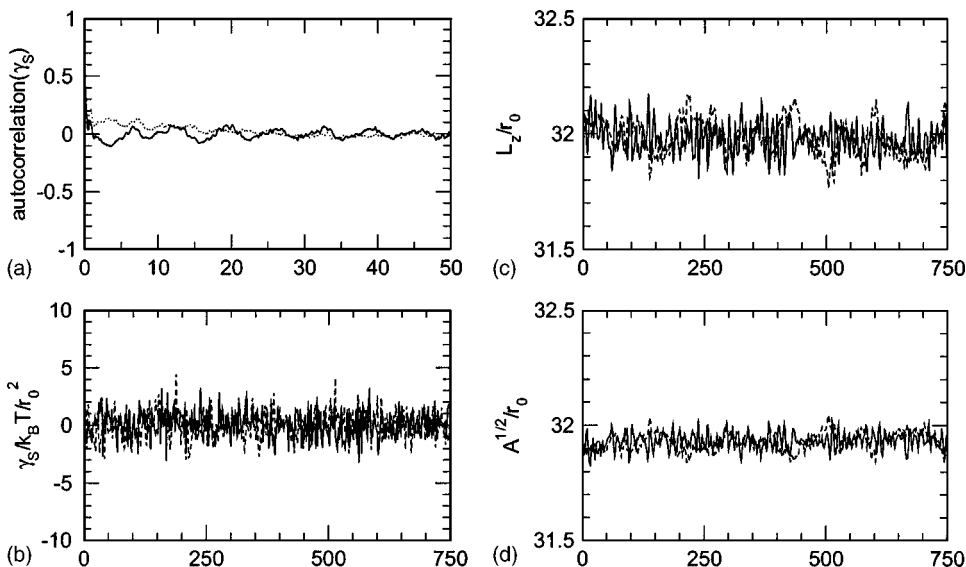


FIG. 7. Autocorrelation function of the instantaneous surface tension. The abscissas are in DPD time units. The full lines correspond to the extended system approach and the dashed line correspond to the Langevin piston. (a) Autocorrelation of γ_S . (b) Instantaneous surface tension $\gamma_S(t)$. (c) Box dimension in the z direction L_z . (d) The linear dimension of the xy plane.

$$K_A = \frac{k_B T \langle A \rangle}{\langle \delta A^2 \rangle}. \quad (32)$$

It is found that $K_A = (158 \pm 31) k_B T / r_0^2$. This cannot be compared directly with the findings in Ref. 13, since the authors did not determine the area compressibility modulus for the exact same lipid model with three head beads as above, but for a single head lipid model. In the single head lipid model which has approximately the same bilayer thickness they obtain $K_A = (162 \pm 32) k_B T / r_0^2$.

Using only DPD (no barostat) $\langle k_B T \rangle_t = 0.9994 \pm 0.0002$ and with the Langevin piston $\langle k_B T \rangle_t = 0.9995 \pm 0.0002$. For the extended system $\langle k_B T \rangle_t = 0.9994 \pm 0.0002$. Again it is seen that the barostat methods do not contribute to the integrator-induced deviation of $\langle k_B T \rangle_t$ from $k_B T$, and that the temperature fluctuations are not affected.

In order to investigate the ability of our Langevin piston approach to stabilize a lipid bilayer with a particular nonzero surface tension, a number of simulations were performed where the target surface tension was set to $\gamma_S^0 = \{-10, -5, -2, 0.5, 5, 10\}$ and the normal pressure to $P_N^0 = 23.2 k_B T / r_0^3$. In these cases, the simulations return the average surface tensions values as $\langle \gamma_S \rangle = \{NA, NA, -2.0347 \pm 0.07, 0.55 \pm 0.06, 5.03 \pm 0.06, NA\}$. For $\gamma_S^0 = 10$ the bilayer broke apart due to the large stress in the plane. For $\gamma_S^0 = -10$ the bilayer buckled immediately, and for $\gamma_S^0 = -5$ a long metastable planar state was observed before the bilayer appeared to buckle (this is not conclusive given the length of the simulation).

The average normal pressure was $\langle P_N \rangle = \{NA, NA, 23.200 \pm 0.002, 23.198 \pm 0.004, 23.200 \pm 0.002, NA\}$ in units of $k_B T / r_0^3$. These results therefore clearly demonstrate both the feasibility and the effectiveness of the approach.

It should be noted that for all the results presented above, and for the barostat parameters chosen, the use of the barostat does not require a smaller time step in the integration algorithm.

VII. CONCLUSION

We have presented a method for performing constant-pressure and constant-surface tension simulations in dissipative particle dynamics using a Langevin piston approach. The approach leads to improvements over other approaches in terms of faster equilibration and shorter correlation times of various system variables. In particular, the coupling of the pressure to the system does not require smaller time steps in

the integration of the DPD equations of motion, thereby providing for faster and more efficient simulations.

With the proposed approach we believe that one can turn DPD simulations into a versatile and convenient computer-experimental laboratory for studying complex soft-matter systems, both in equilibrium and out of equilibrium. In the case of lipid membrane systems, the approach should allow for studies of, for example, phase-separation dynamics, enzymatic remodeling of bilayers, as well as dynamics of lipid-protein interactions.

ACKNOWLEDGMENTS

MEMPHYS-Center for Biomembrane Physics is supported by the Danish National Research Foundation. The author would like to thank Ole G. Mouritsen for his valuable advice and the many discussions concerning the manuscript. The simulations were carried out at the Danish Center for Scientific Computing (DCSC).

- ¹H. C. Andersen, *J. Chem. Phys.* **72**, 2384 (1980).
- ²G. J. Martyna, D. J. Tobias, and M. L. Klein, *J. Chem. Phys.* **101**, 4177 (1994).
- ³M. Parrinello and A. Rahman, *Phys. Rev. Lett.* **45**, 1196 (1980).
- ⁴S. E. Feller, Y. Zhang, R. W. Pastor, and B. R. Brooks, *J. Chem. Phys.* **103**, 4613 (1995).
- ⁵W. G. Hoover, *Phys. Rev. A* **31**, 1695 (1985).
- ⁶A. Kolb and B. Dünweg, *J. Chem. Phys.* **111**, 4453 (1999).
- ⁷D. Quigley and M. I. J. Probert, *J. Chem. Phys.* **120**, 11432 (2004).
- ⁸P. J. Hoogerbrugge and J. M. V. A. Koelman, *Europhys. Lett.* **19**, 155 (1992).
- ⁹P. Español and P. Warren, *Europhys. Lett.* **30**, 191 (1995).
- ¹⁰E. G. Flekkøy and P. V. Coveney, *Phys. Rev. Lett.* **83**, 1775 (1999).
- ¹¹S. Yamamoto, Y. Maruyama, and S. Hyodo, *J. Chem. Phys.* **116**, 5842 (2002).
- ¹²R. D. Groot and K. L. Rabone, *Biophys. J.* **81**, 725 (2001).
- ¹³J. C. Shillcock and R. Lipowsky, *J. Chem. Phys.* **117**, 5048 (2002).
- ¹⁴G. Besold, I. Vattulainen, M. Karttunen, and J. M. Polson, *Phys. Rev. E* **63**, 7611 (2000).
- ¹⁵I. Vattulainen, M. Karttunen, G. Besold, and J. Polson, *J. Chem. Phys.* **116**, 3967 (2002).
- ¹⁶P. Nikunen, M. Karttunen, and I. Vattulainen, *Comput. Phys. Commun.* **153**, 407 (2003).
- ¹⁷M. Venturoli and B. Smit, *PhysChemComm* **2**, 45 (1999).
- ¹⁸M. E. Tuckerman, C. J. Mundy, and G. J. Martyna, *Europhys. Lett.* **45**, 149 (1999).
- ¹⁹M. E. Tuckerman, Y. Liu, G. Ciccotti, and G. J. Martyna, *J. Chem. Phys.* **115**, 1678 (2001).
- ²⁰C. W. Gardiner, *Handbook of Stochastic Methods* (Springer, Berlin, 1983).
- ²¹G. J. Martyna, M. E. Tuckerman, D. J. Tobias, and M. L. Klein, *Mol. Phys.* **87**, 1117 (1996).
- ²²R. D. Groot and P. B. Warren, *J. Chem. Phys.* **107**, 4423 (1997).
- ²³M. P. Allen and D. J. Tildesley, *Computer Simulation of Liquids* (Oxford University Press, New York, 1989).
- ²⁴S. E. Feller and R. W. Pastor, *J. Chem. Phys.* **111**, 1281 (1999).